Food Bioprocess Technol
DOI 10.1007/s11947-008-0129-z

ORIGINAL PAPER

Modeling of Batch Dryers for Shrinkable Biological Materials

Cristina Ratti · Guillermo H. Crapiste

Received: 6 February 2008 / Accepted: 25 July 2008

Abstract Design of dryers for biological materials is a complex problem, since in order to solve the model equations, foodstuff physicochemical and equilibrium properties and drying kinetics should be included as a function of water content and operating variables. Shrinkage of biological materials under dehydration must also be taken into account when the macroscopic balances in the bed of drying need to be solved. The main objective of this work was thus to develop a realistic simulation model to predict batch deep bed drying of shrinkable biological materials. Differential macroscopic balances for heat and mass transfer in the air and solid phases were expressed in moving coordinates in order to solve the problem of particle shrinkage during drying. The equation system was solved by the 'method of lines' using the Gear package for temporal derivatives and finite differences for spatial ones. All the parameters and physical properties required to solve the model were taken from literature or determined independently in lab-scale experiments. A pilot-scale hot air batch dryer was built in order to carry out experimental determinations during drying of slices or cylinders of potato, apple, and carrot at diverse hot air conditions. The appropriate choice of numerical method and initial conditions gave a reliable and stable solution of the equation system. The simulation results agreed closely to experimental data on deep bed batch drying of food particles under different conditions. The use of variable porosity and volume due to shrinkage during drying improved notably the predictions of the simulation model.

Keywords Batch dryer · Heat and mass transfer modeling · Shrinkage · Fruits and vegetables

Written for presentation at the 2007 CIGR Section VI International Symposium on Food and Agricultural Products: Processing and Innovations, Naples, Italy, 24–26 September 2007.

C. Ratti (✉)
Dépt. des sols et de genie agroalimentaire, Université Laval, Québec, Canada
e-mail: Cristina.Ratti@sga.ulaval.ca

G. H. Crapiste
PLAPIQUI,
Camino Carrindanga km. 7,
Bahia Blanca 8000, Argentina

Nomenclature

a_v	particle area/volume (m^{-1})
a_w	water activity (–)
A, B	constants of Eq. 19
Bi_{md}	Biot number for mass transfer (dry zone, –)
c_1, c_3	constants of Eq. 17
C, D, E, F	constants of Eq. 20
Cp_{hs}	specific heat of wet solids (J/kg C)
Cp_{ha}	humid air heat (J/kg C)
D_c	drying chamber diameter (m)
G, H, J, K	constants of Eq. 21
G'	mass air flow rate per area unit (kg/m^2 s)
G_e	air flow rate caused by shrinkage (kg/s)
G_s	air flow rate (kg/s)
h_g	heat transfer coefficient (J/m^2 s C)
$j_H = (h_g/Cp_{ha}\ G_s)\ Pr^{2/3}$	Colburn factor for heat transfer (–)
$j_M = (k_g\ P_{ml}\ M_m/G_s)\ Sc^{2/3}$	Colburn factor for mass transfer (–)
k_g	mass transfer coefficient (kg/kPa m^2 s)
L_o	initial bed height (m)
M_m	air molecular weight (kg/mol)
m_s	dried mass (kg)
n_w	water flux (kg water/s m^2)

NN	step number (–)
P_{ml}	logarithmic average pressure (Pa)
Pr	Prandtl number (–)
p_{ws}	water vapor pressure at saturation (kPa)
$p_{w\infty}$	water vapor pressure (kPa)
q_1, q_2, q_3	constants of Eqs. 17 and 18
Re'	Reynolds number (–)
S	cross-sectional area (m^2)
Sc	Schmidt number (–)
t	time (s)
T_s	solid temperature (°C)
T_g	air temperature (°C)
v_s	air velocity induced into the control volume by the shrinkage phenomenon (m/s)
v_s*	speed of the solids entering the control volume due to shrinkage (m/s)
V	real volume (m^3)
V_l	bed volume (m^3)
x	spatial coordinate (m)
X	water content (dry basis, kg water/kg dry solid)
Y	absolute humidity (kg water/kg dry air)
Y_{sat}	absolute humidity at the saturation point (kg water/kg dry air)

Greeks

ΔH_s	heat of sorption (J/kg)
ΔH_w	vaporization heat (J/kg)
ε	porosity (–)
Φ	generalized drying parameter, Eqs. 15 and 16
λ	moving coordinate (–)
$\Lambda = \lambda/L_o$	dimensionless moving coordinate (–)
μ	air viscosity (Pa s)
ρ_a	air density (kg/m^3)
ρ_s	dry solids density (kg/m^3)

Subscripts

o	initial
m	average
Λ	equation based on moving coordinate Λ (not on fixed coordinate)

Introduction

Most of drying operations related to particulate materials lie under the classification of batch drying (Mujumdar 2006). Design of batch dryers is thus of great importance for industry and also the starting point in the development of other more complex dryer designs, such as that for continuous band dryer. In general, fixed bed batch dryers are appropriate for solids having a defined structure before drying (Heldman and Singh 1981). One of the main problems with this type of dryer is obtaining a uniform moisture distribution in the fixed bed at the end of drying. This is due to the lack of uniformity of the air flow rate through the bed as well as of the temperature and humidity in each place.

Figure 1 shows a schematic of the fixed bed dryer. Four heat and mass transfer equations are needed to represent the design of a batch dryer and, when solved, will give information about moisture and temperature of the product, humidity, and temperature of the air during hot air drying. These four variables are function of time and position in the dryer.

Batch drying design for grains and nuts received an important attention in the literature. Many analytical and empirical models have been developed, predicting closely the experimental data on batch drying of wheat, walnuts, barley, paddy rice, etc. (Izadifar et al. 2006; Basirat-Tabrizi et al. 2002; Devahastin and Mujumdar 1999; Sun and Woods 1997; Farkas and Rendik 1996; Rumsey 1991; Giner et al. 1996; Bakker-Arkema et al. 1974). However, since nuts and grains have minimal shrinkage during drying, these models have been developed with the consideration of constant porosity, particle, and bed volume. Other common, although doubtful, consideration is that time derivatives for air humidity and air temperature are negligible, and thus, they are not considered in many dryer models.

For high-moisture products, such as fruits and vegetables, the supposition of negligible shrinkage is no longer valid when building the model of a fixed bed batch dryer. Many articles in the literature have shown that not only individual high-moisture food particles suffer extensive

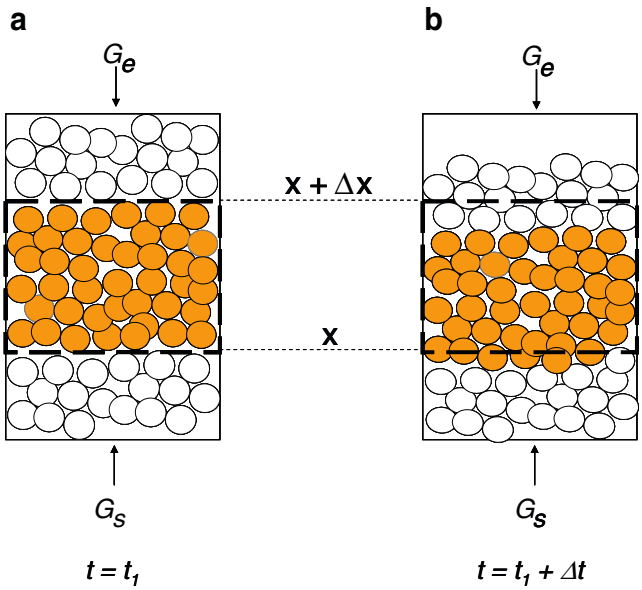

Fig. 1 Control volume in the fixed bed dryer at two drying times, t_1 (**a**) and $t_1+\Delta t$ (**b**)

shrinkage (up to 80%) but also shrinkage affects markedly the bed volume and porosity during drying (Ratti 1994). There are some fixed bed batch dryer models in the literature considering shrinkage (Mabrouk et al. 2006; Karim and Hawlader 2005; García-Alvarado and Herman-Lara 2004; Ratti and Mujumdar 1995). However, some of the previous articles take into account only the shrinkage of single particles in order to evaluate the drying kinetics, not considering the change in porosity and bed length during drying (Mabrouk et al. 2006; Karim and Hawlader 2005). Others do consider the change in bed length and particle size due to shrinkage by evaluating the average between the final and initial bed length values, but without changing appropriately the macroscopic heat and mass transfer model equations with time (García-Alvarado and Herman-Lara 2004). Ratti and Mujumdar (1995) include shrinkage of the particle as well as that of bed length and porosity in their mathematical model by transforming the coordinates from fixed to moving ones. However, this model was used to study airflow reversal in the fixed bed (Ratti and Mujumdar 1995) or for predicting solar drying (Ratti and Mujumdar 1997). No comparison of the model predictions to actual drying data in a fixed bed dryer, or of discussion of the effect of shrinkage on these predictions, has been reported so far.

The main goal of the present work was to analyze how shrinkage should be taken into account for modeling fixed bed drying of food particles. A mathematical heat and mass transfer model was developed for simulation of a shrinking bed of food particles undergoing fixed bed batch drying. The results of the model will be compared to experimental data on batch drying of carrot, potato, and apple particles of different geometries. The effect of considering shrinkage in the proposed model will be discussed and compared to experimental data.

Materials and Methods

Mathematical Model

The mathematical model of a dryer consists in the energy and material differential macroscopic balances for the air and the food particles. In the fixed batch bed dryer, a differential portion of the fixed bed having Δx thickness was taken as the control volume (Fig. 1). In this control volume, constant air temperature and humidity as well as constant moisture content and temperature of the particles are supposed.

The key suppositions in the development of this model were:

(a) Air flow distribution is uniform in the bed cross-section.
(b) The system is adiabatic; thus, there are no energy losses through the dryer walls.
(c) The predominant mechanism of heat transfer for the solid particles is external (convection).
(d) Conduction heating and contact diffusion between particles are negligible.

When describing mathematically the heat and mass balances for the solids and the air, it is important to note that, as shown schematically in Fig. 1 for two different drying times, there is a flow of solids and air inside the control volume due to the shrinkage (air flow due to shrinkage is marked as G_e in Fig. 1), which takes place in the opposite direction of the main air flow G_s. Taking into account the previous consideration, the microscopic heat and mass balances in the solids and the air could be written:

Humidity balance in the air:

$$\frac{\partial Y}{\partial t} - v_s \frac{\partial Y}{\partial x} = \frac{n_w\, a_v\, (1-\varepsilon)}{\rho_a\, \varepsilon} - \frac{G_s}{S\, \rho_a\, \varepsilon}\, \frac{\partial Y}{\partial x} \tag{1}$$

Moisture balance in the solids:

$$\frac{\partial X}{\partial t} - v_s^{*} \frac{\partial X}{\partial x} = -\frac{n_w\, a_v}{\rho_s} \tag{2}$$

Energy balance in the solids:

$$\frac{\partial T_s}{\partial t} - v_s^{*} \frac{\partial T_s}{\partial x} = \frac{a_v}{\rho_s (1+X) Cp_{hs}} \left[h_g \left(T_g - T_s\right) - n_w\, \Delta H_s\right] \tag{3}$$

Energy balance in the air:

$$\frac{\partial T_g}{\partial t} - v_s \frac{\partial T_g}{\partial x} = -\frac{h_g\, a_v\, (1-\varepsilon)}{\rho_a\, \varepsilon\, Cp_{ha}} \left(T_g - T_s\right) - \frac{G_s}{\rho_a\, \varepsilon\, S}\, \frac{\partial T_g}{\partial x} \tag{4}$$

In Eqs. 1, 2, 3, and 4, v_s^{*} represents the speed of the solids entering the control volume due to shrinkage and v_s, the air velocity induced also by the shrinkage phenomenon:

$$v_s = \frac{G_e}{S\, \varepsilon\, \rho_a} \tag{5}$$

The problem of shrinkage in the bed of particles during drying can be undertaken by a suitable change from fixed to moving coordinates. The material coordinates of a particle place its position in a reference configuration (Slattery 1981). In this work, a differential volume element is defined as the one that contains always the same amount of dried material and for which the reference configuration is the dried material at the initial time. From this, we can define the new material coordinate:

$$t = 0 \qquad dm_{s,o} = \rho_{s,o}\ \ (1-\varepsilon_o)\ S\, d\lambda \tag{6}$$

$$t = t \qquad dm_s\ \ = \rho_s\, (1-\varepsilon)\, S\, dx. \tag{7}$$

The selected element will be the one having $dm_s = dm_{s,o}$. Thus, the reduced dimensionless coordinate (i.e., $\Lambda = \lambda/L_o$) is:

$$d(x/L_o) = \frac{\rho_{s,o}(1-\varepsilon_o)}{\rho_s(1-\varepsilon)} d\Lambda. \tag{8}$$

In these new material coordinates, the microscopic balances in the deep bed result in:

Humidity balance in the air:

$$\left[\frac{\partial Y}{\partial t}\right]_\Lambda = \frac{n_w\, a_v\,(1-\varepsilon)}{\rho_a\,\varepsilon} - \frac{1}{S\,L_o}\,\frac{G_s}{\rho_a\,\varepsilon}\,\frac{\rho_s\,(1-\varepsilon)}{\rho_{s,o}\,(1-\varepsilon_o)}\,\frac{\partial Y}{\partial \Lambda} \tag{9}$$

Moisture balance in the solids:

$$\left[\frac{\partial X}{\partial t}\right]_\Lambda = -\frac{n_w\, A_v}{\rho_s} \tag{10}$$

Energy balance in the solids:

$$\left[\frac{\partial T_s}{\partial t}\right]_\Lambda = \frac{a_v}{\rho_s\,(1+X)\,Cp_{hs}}\,\left[h_g\left(T_g - T_s\right) - n_w\,\Delta H_s\right] \tag{11}$$

Energy balance in the air:

$$\left[\frac{\partial T_g}{\partial t}\right]_\Lambda = -\frac{h_g\, a_v\,(1-\varepsilon)}{\rho_a\,\varepsilon\,Cp_{ha}}\,\left(T_g - T_s\right) - \frac{1}{S\,L_o}\,\frac{G_s}{\rho_a\,\varepsilon} \times \frac{\rho_s\,(1-\varepsilon)}{\rho_{s,o}\,(1-\varepsilon_o)}\,\frac{\partial T_g}{\partial \Lambda}. \tag{12}$$

The previous model will be solved with the following initial conditions:

$$\Lambda = 0 \begin{cases} X = X_o \\ T_s = T_{so} \\ Y = Y_o \\ T_g = T_{go} \end{cases} \qquad \Lambda \neq 0 \begin{cases} X = X_o \\ T_s = T_{so} \\ Y = Y_{sat}\,(T_{so}) \\ T_g = T_{so} \end{cases} \tag{13}$$

where, at $\Lambda \neq 0$, air conditions were estimated as those in equilibrium with the solid.

A border condition is also needed to solve the previous equation system (Eqs. 9, 10, 11, and 12):

$$\Lambda = 0 \qquad \Rightarrow \qquad T_g = T_{go} \;\text{ and }\; Y = Y_o. \tag{14}$$

Prior to solving the equation system (Eqs. 9, 10, 11, and 12), many parameters and physical properties should be evaluated or estimated. In this model, no parameter was fitted from the experimental data obtained in packed bed drying (see description of the experiments later). All the parameters and physical properties required to solve the model were taken from literature, determined independently in lab-scale experiments.

The water flux corresponding to the drying kinetics of a single particle was estimated using a semi-theoretical model previously developed (Ratti and Crapiste 1992; Fontaine and Ratti 1999):

$$n_w = \frac{k_g[a_w\, p_{ws}(T_s) - p_{w\infty}]}{\left[1 + \left(\Phi/X_o\right) Bi_{md}\right]} \tag{15}$$

where the parameter Φ for carrot, apple, and potato particles of different geometries can be taken from the following expression (Ratti and Crapiste 1992):

$$\Phi \;=\; 0.00532(X/X_o)^{-1.079}. \tag{16}$$

Water activity was determined from the expression developed by Ratti et al. (1989):

$$\ln a_w = -c_1\, X^{c_3} + q_1 \quad \exp\left(-q_2\, X\right) X^{q_3} \quad \ln p_{ws} \tag{17}$$

where parameters c_1, c_3, q_1, q_2, and q_3 for apple, potato, and carrot can be found in Table 1. Heat of sorption was thus calculated from:

$$\Delta H_s = \left[1 + q_1\, \exp\left(-q_2\, X\right) X^{q_3}\right]\, \Delta H_w \tag{18}$$

Specific heat of solids was obtained from the following expression (Ratti and Crapiste 1995):

$$Cp_{hs} = A + B\,\left(\frac{X}{1+X}\right) \tag{19}$$

where parameters A and B can be found in Table 1 for potato, apple, and carrot.

The particle specific area (area/volume), bed volume, and porosity can be estimated by using Eqs. 20, 21, and 22 (Ratti 1994):

$$a_v/a_{vo} = C \;\; + \; D\;(X/X_o) + E\;(X/X_o)^2 + F\;(X/X_o)^3 \tag{20}$$

$$V_1/V_{lo} = G + H(X/X_o) + J(X/X_o)^2 + K(X/X_o)^3 \tag{21}$$

$$\varepsilon = 1 - V/V_1 \tag{22}$$

The parameters C, D, E, F, G, H, J, and K are presented in Table 1 for apple, potato, and carrot and for different geometries.

Finally, the heat transfer coefficient in the drying bed with through circulation of air was approximated from the following equation (Bradshaw and Myers 1963):

$$j_M = 2.25\; Re'^{\,-0.501} \;\;,\;\; 300 < Re' < 3{,}000 \;\;,\;\; j_H/j_M = 1.12 \tag{23}$$

where j_M and j_H are the mass and heat transfer Colburn factors and $Re' = (D_c\, G')/(\mu(1-\varepsilon))$. G' is the air mass flow

Table 1 Constants used in the estimation of several properties necessary in the dryer design

Constant	Foodstuff					
	Potato		Apple		Carrot	
	Cylinders	Slices	Cylinders	Slices	Cylinders	Slices
A[a]	1.612		1.733		1.737	
B[a]	3.114		2.382		2.340	
C[b]	2.175	2.952	1.916	1.854	2.553	3.293
D[b]	−3.194	−6.683	−1.921	−1.845	−4.888	−8.600
E[b]	3.661	8.639	1.595	1.660	2.877	11.913
F[b]	−1.661	−3.938	−0.596	−0.678	−1.029	−5.653
c_1[c]	0.0267		0.182		0.170	
c_3[c]	−1.656		−0.696		−0.720	
q_1[c]	0.0107		0.232		0.0565	
q_2[c]	1.287		43.943		0.0835	
q_3[c]	−1.513		0.0411		1.547	
G[b]	0.339		0.390		0.335	
H[b]	1.246		1.031		0664	
J[b]	−1.385		−0.622		0.163	
K[b]	0.792		0.202		−0.168	

[a] Ratti and Crapiste (1995)
[b] Ratti (1994)
[c] Ratti et al. (1989)

rate per area unit before entering the bed, D_c is the cylinder diameter, μ is the air viscosity, and ε the bed porosity.

Method of Resolution

Numerical resolution of heat and mass balances (Eqns. 9, 10, 11, 12) was done using the numerical method of lines. Temporal derivatives corresponding to air humidity and temperature, and particle temperature and moisture, were solved using the Gear routine (Hindmarsh 1974). Spatial derivatives were solved by finite differences. The bed was divided in *NN* steps; thus, the problem resulted in a vector of four (*NN*+1) equations. The Gear routine solved four differential equations for each line in an implicit way (at a distance Λ).

At Λ=0, the temporal derivatives of air temperature and humidity were fixed as 0 in order to maintain constant the condition of the air at the inlet of the dryer. On the other hand, for $\Lambda \neq 0$, spatial derivatives discretization was done by backward finite differences in order to avoid hypothetical conditions for the air at the exit of the dryer.

Experimental Beds of Food Particles

White potato, red delicious apple, and carrot were used in the drying experiments. They were cut in cylinders (1-cm diameter by 5-cm length cylinders) or slices (5-cm diameter by 0.9-cm thickness). Particle beds containing between 140 and 200 cylinders, or 60 to 80 slices, of potato, carrot, and apple were formed for the drying experiments.

Drying Experiments

A pilot-scale batch dryer was built with air flowing through the particle bed. The main parts of this dryer are shown in Fig. 2. The dryer had a root-type compressor to move the air. Air flow rate could be controlled by a valve calibrated with the average air velocity achieved in the drying chamber. The batch dryer worked in a closed loop. Air was heated to the desired temperature by passing it through a set of calibrated heating elements and controlled with an on–off controller. Relative humidity could be controlled by passing the mass of air through a saturation chamber where saturated salt solutions were sprayed continuously over the flowing air. Air leaving the saturation chamber had the relative humidity of the salt solution that was being sprayed and could be kept constant throughout the drying experiment since the system worked in a closed loop. Then, the air entered the cylindrical drying chamber (made of 0.8-cm-thick Plexiglas) and passed through a series of deflectors, which were placed before the cylindrical drying bed (also made in 0.8-cm-thick Plexiglas but with a screened bottom) to uniform the velocity distribution and thus to obtain a flat profile (plug flow) in the drying bed.

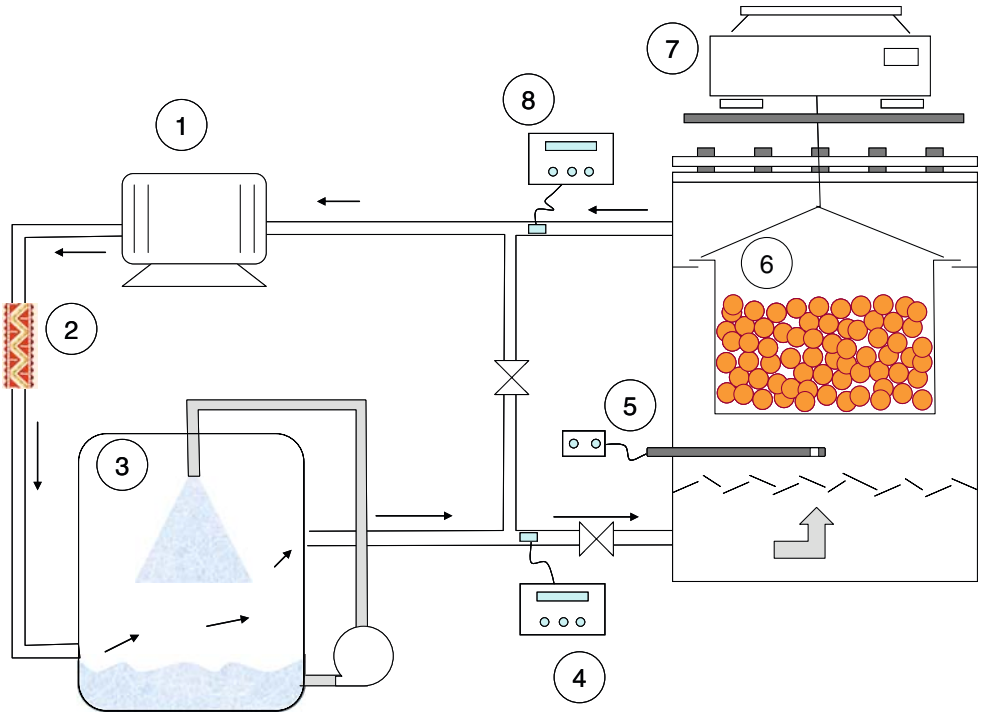

Fig. 2 Schematic of the pilot-scale batch dryer. *1* Root compressor, *2* Electrical heating elements, *3* Saturation chamber, *4* Temperature and relative humidity sensors (air inlet), *5* Anemometer, *6* Drying chamber, *7* Balance, *8* Temperature and relative humidity sensors (air exit)

Weight measurements were done at predetermined times in discontinuous mode using a balance placed on top of the drying chamber, with deviation of the air through a valve system in order to avoid erroneous measurements due to air flow. Dried mass was obtained in a vacuum oven during 72 h at 60 °C using $CaCl_2$ as desiccant.

Temperature and relative humidity were measured entering and leaving the drying chamber using K-type thermocouples and a Vaisala humidity sensor. Temperature of the experiments was set at approximately 50 °C or 60 °C, and relative humidity was 33% (corresponding to a saturated solution of $MgCl_2$). Air velocity entering the drying chamber was measured using an anemometer. Averaged air velocities ranged between 0.1 and 3 m/s.

Bed thickness was obtained as the average of the height measured on graduated scales placed on the side of the drying chamber at three different positions. Bed apparent volume was calculated by multiplying the averaged bed height by the cross sectional area (Ratti 1994). The initial bed length varied between 3.5 and 5.5 cm.

Results and Discussion

The number of the integration steps, *NN*, was optimized to ten in order to obtain a convergent strong solution in a minimal time. Water content, air humidity, solid and air temperatures (X, Y, T_s, and T_g, respectively) were obtained as a function of the dimensionless space moving coordinate, Λ, and of time, t. The average water content in the bed at each time, $(X/X_o)_m$, was obtained from the following calculation:

$$(\mathrm{X}/\mathrm{X_o})_\mathrm{m} = \left(\sum_{i=1}^{NN} (\mathrm{X}/\mathrm{X_o})_i\right) (1/NN) \tag{24}$$

A comparison was carried out between the model predictions (Eqs. 9, 10, 11, and 12) and the experimental data of drying of potato slices (Fig. 3). Model simulation of the average water content in the drying bed had a close agreement to the experimental pilot-scale data. Figure 3 also includes the comparison of the model predictions when no shrinkage is considered (dotted line). The comparison points out that if shrinkage is not taken into account, the model values are much smaller than experimental ones, and drying seems faster. This is certainly due to the fact that surface area is an important parameter for mass transfer. Therefore, if no shrinkage occurs, the available surface area would be bigger and moisture would be lost more rapidly. From the model predictions, it can be derived that 200 min is required to dry the bed of potato slices if shrinkage is not considered. However, experimental data and model predictions considering shrinkage confirmed that the actual drying time is approximately 450 min. This comparison was done for other food products and geometries, giving similar results. This clearly demonstrates that shrinkage should not be neglected when modeling heat and mass transfer during drying of high moisture foods in deep beds.

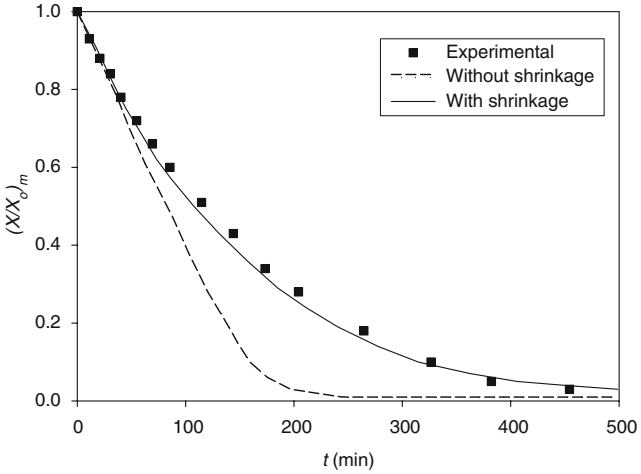

Fig. 3 Bed average moisture content during drying of potato slices at 50 °C and 1.75 m/s: *square*, experimental data; *dashed line*, model without shrinkage; *solid line*, model with shrinkage

The average water content and the exit air temperature were recorded during drying of apple cylinders at two inlet air temperatures, 62.5 °C and 47.8 °C (Fig. 4). As expected, drying was faster at higher inlet temperatures. Its takes approximately 200 min to complete drying at 62.5 °C, while for 47.8 °C, the drying time is 75% longer. The model predicts with accuracy the average water content as well as the exit air temperature at varying inlet conditions.

The average bed drying curves of apple particles having different geometries (cylinders and slices) were recorded (Fig. 5). Particle geometry is an important variable for drying; thus, it had a marked influence in drying time during the first drying stages. Apple cylinders dry faster than slices; however, the time to achieve complete drying seems to be approximately the same for both types of geometries. Simulation results (Fig. 5) agreed closely to experimental data.

Good agreement between experimental and predicted values was also obtained for slices of different foodstuffs studied in this work such as apple, potato, and carrot (Fig. 6). Most of the comparisons between experimental data and model predictions on batch drying of different particle geometries and foodstuffs were satisfactory. For potato cylinders at different air velocities (Fig. 7), however, the comparison between experimental and prediction values is acceptable, although the model seems to approximate better the experimental points at high air velocities used in the dryer, i.e., when mass transfer internal control is predominant. This could be due to the use of a heat transfer coefficient (Eq. 16) which has been taken directly from literature and not developed specifically for this dryer configuration. However, the predictions are acceptable.

The proposed model can serve to understand more deeply the behavior of packed beds (thin or deep) during

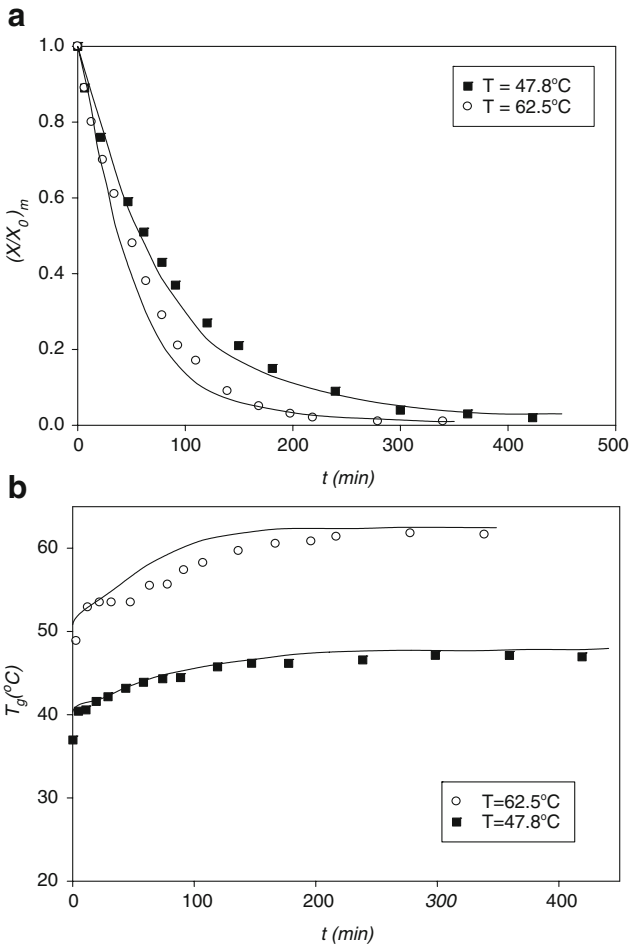

Fig. 4 Bed average moisture content (**a**) and exit air temperature (**b**) during drying of apple cylinders at 0.8 m/s and inlet drying air temperatures of 62.5 °C (*circle*) and 47.8 °C (*square*), model (*solid line*)

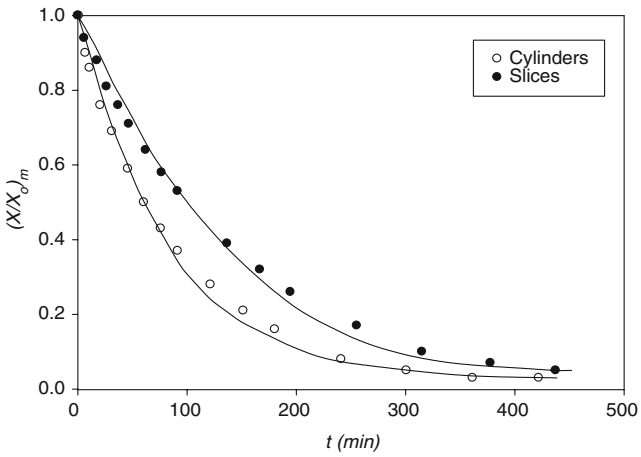

Fig. 5 Average moisture content during drying of apple cut in cylinders (*filled circle*) at T=47.8 °C and v=0.8 m/s, or in slices (*open circle*) at 49 °C and 1.04 m/s, model (*solid line*)

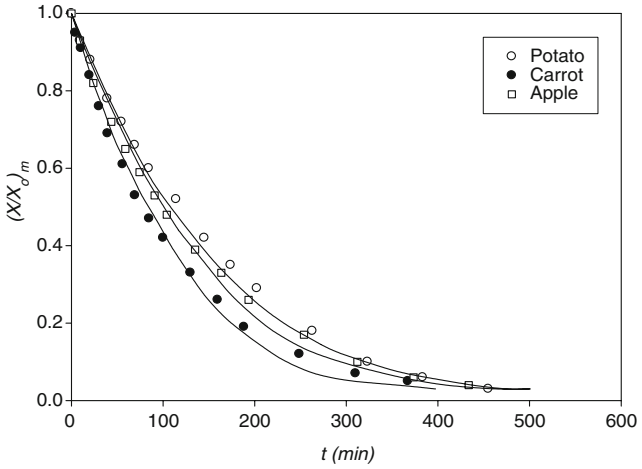

Fig. 6 Average moisture content during drying of slices of carrot (*filled circle*) at T=49.7 °C and v=2.1 m/s, apple (*square*) at 49 °C and 1.0 m/s, and potato (*open circle*) at 50 °C and 1.75 m/s, model (*solid line*)

hot air batch drying of foodstuffs. Figure 8 shows the simulation results of moisture and temperature profiles for potato slab drying at two bed heights (5 and 30 cm). As can be seen, increasing the bed height has a marked impact on drying and temperature profiles. From these results, non-uniform moisture distribution in the final product and bad energy efficiency (due to increased temperature difference between the bottom and the top of the drying bed) could be expected at higher bed heights. The results could be extended to predict air humidity and temperature profiles (not shown), which could be certainly useful in dryers with air recirculation.

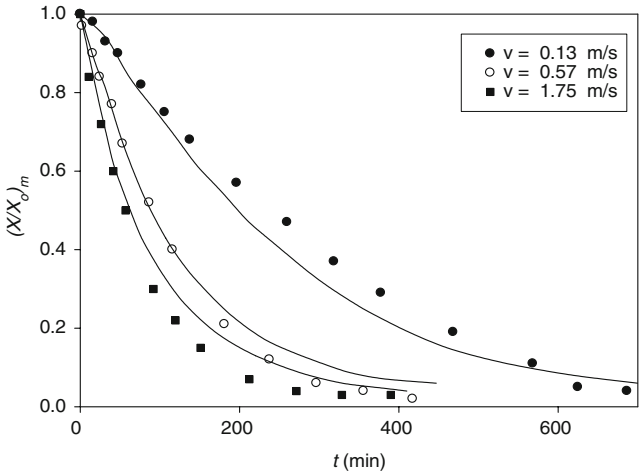

Fig. 7 Bed average moisture content during drying of potato cylinders at 60 °C and inlet drying air velocity of v=1.75 m/s (*filled square*), 0.57 m/s (*open circle*), and 0.13 m/s (*filled circle*), model (*solid line*)

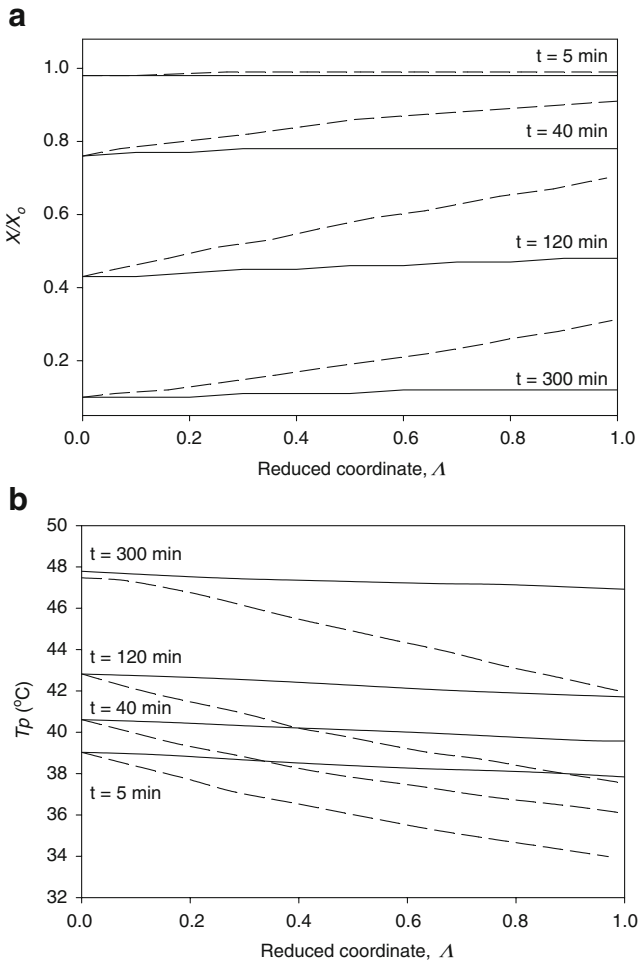

Fig. 8 Simulation results on moisture (**a**) and temperature (**b**) profiles in the dryer bed at different times during drying of potato slabs at 50 °C and 3 m/s: 30-cm bed height (*dashed line*) and 5-cm bed height (*solid line*)

Conclusions

A model to represent heat and mass transfer of shrinkable food particles in a batch dryer was developed. All the parameters and physical properties required to solve the model were determined independently from the packed bed dryer experiments (in lab-scale experiments) or taken from literature. A pilot-scale hot air batch dryer was built in order to carry out experimental determinations during packed bed drying of slices or cylinders of potato, apple, and carrot at diverse hot air conditions.

The appropriate choice of numerical method and initial conditions gave a reliable and stable solution of the equation system. The simulation results agreed closely to experimental data on deep bed batch drying of apple, carrot, and potato particles under different air and particle conditions. The use of variable porosity and volume due to shrinkage during drying improved notably the predictions

of the simulation model, showing that shrinkage should not be neglected in the modeling.

Acknowledgments The authors would like to acknowledge the financial support of CONICET (Consejo Nacional de Investigaciones Cientificas y Tecnicas, Argentina) and NSERC (National Science and Engineering Research Council, Canada).

References

Bakker-Arkema, F. W., Farmer, D. M., & Lerew, 1. E. (1974). Optimum grain dryer design through simulation. *Annales de Technologie Agricole*, *22*(3), 275–290.

Basirat-Tabrizi, H., Saffar-Avval, M., & Assarie, M. R. (2002). Two-dimensional mathematical model of a packed bed dryer and experimentation. *Proceedings of the Institution of Mechanical Engineers, Part A: Journal of Power and Energy*, *216*(2), 161–168.

Bradshaw, R. D., & Myers, J. E. (1963). Heat and mass transfer in fixed and fluidized beds of large particles. *AIChE Journal*, *9*(5), 590–595. doi:10.1002/aic.690090505.

Devahastin, S., & Mujumdar, A. S. (1999). Batch drying of grains in a well-mixed dryer-effect of continuous and stepwise change in drying air temperature. *Transactions of the ASAE*, *42*(2), 421–425.

Farkas, I., & Rendik, Z. (1996). Block oriented modeling of drying processes. *Mathematics and Computers in Simulation*, *42*, 213–219. doi:10.1016/0378-4754(96)00003-1.

Fontaine, J., & Ratti, C. (1999). Lumped-parameter approach for prediction of drying kinetics in foods. *Journal of Food Process Engineering*, *22*(4), 287–305. doi:10.1111/j.1745-4530.1999.tb00486.x.

García-Alvarado, M. A., & Herman-Lara, E. (2004). Drying of food with sorption isotherms calculated by Ross equation. *Drying Technology*, *22*(9), 2051–2064. doi:10.1081/DRT-200034211.

Giner, S. A., Mascheroni, R. H., & Nellist, M. E. (1996). Cross-flow drying of wheat: A simulation program with a diffusion-based deep-bed model and a kinetic equation for viability loss estimation. *Drying Technology*, *14*(10), 2255–2292. doi:10.1080/07373939608917206.

Heldman, D. R., & Singh, R. P. (1981). *Food process engineering, 2nd ed*. New York, USA: AVI/Van Nostrand Reinhold.

Hindmarsh, A. C. (1974). *Gear: Ordinary differential equation system solver. Technical Report UCID-30001, ReD. 3*. Livermore, CA, USA: Lawrence Livermore Laboratory.

Izadifar, M., Baik, O., & Simonson, C. (2006). Modeling of the packed bed drying of paddy rice using the local volume averaging (LVA) approach. *Food Research International*, *39*, 712–720. doi:10.1016/j.foodres.2006.01.009.

Karim, A., & Hawlader, M. N. A. (2005). Drying characteristics of banana: Theoretical modeling and experimental validation. *Journal of Food Engineering*, *70*, 35–45. doi:10.1016/j.jfoodeng.2004.09.010.

Mabrouk, S. B., Khiari, B., & Sassi, M. (2006). Modelling of heat and mass transfer in a tunnel dryer. *Applied Thermal Engineering*, *26*, 2110–2118. doi:10.1016/j.applthermaleng.2006.04.007.

Mujumdar, A. S. (2006). *Handbook of industrial drying, 3rd ed*. New York, USA: CRC.

Ratti, C. (1994). Shrinkage during drying of foodstuffs. *Journal of Food Engineering*, *23*(1), 91–105. doi:10.1016/0260-8774(94)90125-2.

Ratti, C., & Crapiste, G. H. (1992). A generalized drying curve for hygroscopic shrinking materials. In A. S. Mujumdar (ed.) Drying'92, vol. 1 (pp. 864–874). London: Elsevier.

Ratti, C., & Crapiste, G. H. (1995). Determination of heat transfer coefficients during drying. *Journal of Food Process Engineering*, *18*(1), 41–53. doi:10.1111/j.1745-4530.1995.tb00353.x.

Ratti, C., Crapiste, G. H., & Rotstein, E. (1989). A new water sorption equilibrium expression for solid foods based on thermodynamic considerations. *Journal of Food Science*, *54*(3), 738–742. doi:10.1111/j.1365-2621.1989.tb04693.x.

Ratti, C., & Mujumdar, A. S. (1995). Simulation of flow reversal drying in a packed bed. *Journal of Food Engineering*, *26*(3), 259–271. doi:10.1016/0260-8774(94)00007-V.

Ratti, C., & Mujumdar, A. S. (1997). A mathematical model for solar batch drying of carrots. *Solar Energy Journal*, *60*(3–4), 151–157. doi:10.1016/S0038-092X(97)00002-9.

Rumsey, T. (1991). Modeling moisture variability in a fixed-bed dryer. *Dry Technology*, *9*(1), 61–78. doi:10.1080/07373939108916641.

Slattery, J. C. (1981). *Momentum, energy, and mass transfer in continua*. Huntington, New York, USA: R.E. Krieger.

Sun, D. W., & Woods, J. L. (1997). Simulation of the heat and moisture transfer process during drying in deep grain beds. *Drying Technology*, *15*(10), 2479–2508. doi:10.1080/07373939708917371.